

**Electric-quadrupole transition of H<sub>2</sub> determined to 10<sup>-9</sup> precision**C.-F. Cheng(程存峰),<sup>1</sup> Y. R. Sun(孙羽),<sup>1</sup> H. Pan(潘虎),<sup>1</sup> J. Wang(王进),<sup>1</sup> A.-W. Liu(刘安雯),<sup>1</sup>  
A. Campargue,<sup>2</sup> and S.-M. Hu(胡水明)<sup>1,\*</sup><sup>1</sup>Hefei National Laboratory for Physical Sciences at Microscale, University of Science and Technology of China, Hefei 230026, China<sup>2</sup>Université Grenoble I/CNRS, UMR5588 LIPhy, Grenoble F-38041, France

(Received 9 January 2012; published 6 February 2012)

The  $S(3)$  electric-quadrupole transition of the (3-0) overtone of molecular hydrogen has been recorded with a continuous-wave cavity ring-down spectrometer and calibrated with sub-megahertz accuracy using a temperature-stabilized Fabry-Pérot interferometer. The collision-induced frequency shift and the frequency at zero pressure limit are derived from a fit of the spectral profiles. The absolute transition frequency of the  $S(3)$  line is determined to be 376 531 818.1 MHz with a 1.6-MHz accuracy ( $\delta\nu/\nu = 4 \times 10^{-9}$ ) by measuring the shift to a Rb line at 795 nm. As the best determined transition frequency of neutral H<sub>2</sub> in the ground electronic state, this value agrees well with recent high-level quantum chemistry calculations including relativistic and quantum electrodynamics corrections.

DOI: 10.1103/PhysRevA.85.024501

PACS number(s): 33.20.Ea, 31.30.J-

The hydrogen molecule, the smallest neutral molecule, is a particularly interesting test ground of chemical bonding theories and precise quantum chemistry calculations. *Ab initio* calculations, including nonadiabatic, relativistic, and quantum electrodynamics (QED) corrections, have recently been applied to calculate the H<sub>2</sub> dissociation energy to  $2.7 \times 10^{-8}$  precision [1]. The dissociation energies of H<sub>2</sub>, HD, and D<sub>2</sub> have been experimentally determined by Zhang *et al.* [2] and then improved by Liu *et al.* with 11-MHz accuracy ( $\frac{\delta\nu}{\nu} \simeq 1 \times 10^{-8}$ ) [3–5]. The experimental and calculated results agree within a combined uncertainty of 30 MHz, and can potentially be improved to the sub-megahertz level [6]. Taking into account adiabatic and nonadiabatic effects, a set of rovibrational energies of molecular hydrogen have been calculated [7,8], and an accuracy of 0.001–0.005 cm<sup>-1</sup> has been achieved taking into account QED effects [9]. Recently, the rotational energy levels up to  $J = 16$  of the ( $X^1\Sigma_g^+$ ,  $V = 0$ ) vibronic ground state were experimentally determined to 0.005 cm<sup>-1</sup> accuracy in order to investigate the QED and relativistic contributions [10]. The line positions of H<sub>2</sub> can also be applied to find cosmological variation of the proton-electron mass ratio. A variation at the  $3.5\sigma$  confidence level has been observed by Reinhold *et al.* using the Lyman band lines of H<sub>2</sub> with relative position accuracy of  $5 \times 10^{-8}$  [11].

As a homonuclear diatomic molecule, in general, H<sub>2</sub> has no dipole transition in the rotation-vibration spectrum. However, very weak electric-quadrupole transitions are allowed. Since the first laboratory detection by Herzberg in 1949 [12], extensive studies of the H<sub>2</sub> quadrupole transitions have been carried out from the rotational region to the fourth overtone band (see the recent review included in Ref. [13]). For the second overtone band of H<sub>2</sub> near 0.8 μm, the  $S_3(J)$  ( $\Delta V = 3$ ,  $\Delta J = 2$ ,  $J = 0 - 3$ ) positions have been measured with a relative precision of  $10^{-7}$  by Bragg *et al.* using 2.8-atm hydrogen gas sample and a Fourier-transform spectrometer (FTS) equipped with a 434-m multipass cell (6-m base) [14]. The comparison of their results with the calculated values [9]

show large systematic deviation ( $\sim 10^{-2}$  cm<sup>-1</sup>), mostly due to the pressure shift, which was not determined. More recently, Robie and Hodges reported the  $S_3(J)$  ( $J = 0 - 3$ ) and  $Q_3(J)$  ( $J = 1 - 3$ ) lines by pulsed cavity ring-down spectroscopy (CRDS), but the line positions are reported with 0.02-cm<sup>-1</sup> accuracy [15]. In the present study, the pressure shift and transition frequency of the  $S_3(3)$  transition could be accurately determined using a highly sensitive continuous-wave cavity ring-down spectrometer. Using the <sup>87</sup>Rb atomic line at 795 nm as a frequency reference, the absolute transition frequency of the  $S_3(3)$  transition at 796.2 nm is determined with an accuracy of  $5 \times 10^{-5}$  cm<sup>-1</sup> ( $\frac{\delta\nu}{\nu} = 4 \times 10^{-9}$ ), which is 120 times more accurate than the previous FTS value. As the most accurately determined transition frequency of the neutral hydrogen molecule, this quadrupole transition in the electric ground state provides a good test of the most recent high-level quantum chemistry calculations.

The second overtone band of H<sub>2</sub> was measured at room temperature (296 K) using a cavity ring-down spectrometer based on a continuous-wave Ti:sapphire laser. The ultra-high sensitivity of the spectrometer allows the detection of the very weak  $S_3(3)$  transition with a sufficient signal-to-noise ratio at relatively low sample pressures (200–750 Torr). This has the advantage of limiting the impact of pressure-induced effects on the retrieved line parameters [16]. The configuration of the cavity ring-down spectrometer has been presented in Refs. [17,18]. In brief, the ring-down signal emitted from a high-finesse cavity composed of a pair of mirrors with reflectivity of 0.99995 is detected to retrieve the ring-down time  $\tau(\nu)$ . The sample absorption coefficient  $\alpha(\nu)$  is obtained from

$$\alpha(\nu) = \frac{1}{c\tau(\nu)} - \frac{1}{c\tau_0}, \quad (1)$$

where  $c$  is the speed of light and  $\tau_0$  is the ring-down time of the empty cavity. The minimal detectable (noise-equivalent) absorption coefficient  $\alpha_{\min}$  is  $1 \times 10^{-10}$  cm<sup>-1</sup>.

Sub-megahertz frequency accuracy is achieved by using the Rb atomic line at 795 nm as a frequency standard. The schematic optical layout is shown in Fig. 1. The idea is to use the passive modes of a Fabry-Pérot interferometer (FPI) to

\*smhu@ustc.edu.cn

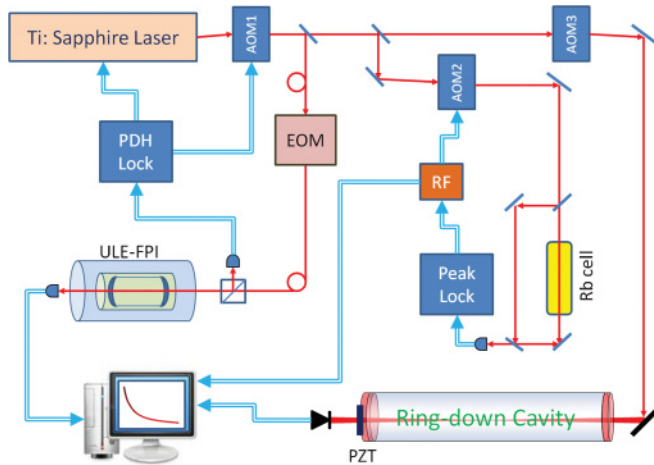


FIG. 1. (Color online) Experimental setup. The abbreviations are as follows: AOM, acousto-optical modulator; EOM, electro-optical modulator; PDH Lock, Pound-Drever-Hall locking; PZT, lead zirconate titanate piezoelectric actuator; RF, radio frequency source driver; ULE-FPI, Fabry-Pérot interferometer made of ultra-low-expansion glass.

transfer the 795-nm frequency standard to 796.2 nm, where the  $S_3(3)$  transition of  $H_2$  is located. The 10-cm-long FPI is made of ultra-low-expansion glass (ULE) and is installed in a vacuum chamber. The ULE-FPI is thermostabilized at about 303 K with a temperature drift below 10 mK during the recordings. A fiber electro-optic modulator (EOM) with 5-GHz bandwidth was used to produce sidebands on the carrier laser. One of the sidebands is locked on a selected longitudinal mode of the ULE-FPI using the Pound-Drever-Hall method. The slow and fast feedback control signals are delivered to the laser controller and an acousto-optical modulator (AOM1), respectively. The carrier laser beam is also locked on the Rb saturation absorption line peak, and the feedback control is accomplished by tuning the radio frequency driving another AOM (AOM2). The Rb vapor cell is installed in a magnetic shield (residual magnetic field  $\simeq 0.2$  mG) to eliminate Zeeman frequency shift due to the magnetic field. In this case, the frequency difference between the Rb line and the selected ULE-FPI mode can be obtained from the radio frequencies driving the fiber EOM and AOM2. The transmittance peaks of the ULE-FPI are indexed with integer numbers, and the one adjacent to the  $^{87}\text{Rb}$  795-nm  $|5^2S_{1/2}, F = 2\rangle \rightarrow |5^2P_{1/2}, F' = 1\rangle$  transition is chosen as  $N = 0$ . The relative frequency shift of the  $N = 0$  peak to the Rb line has been determined to be  $-247.438$  MHz with a standard deviation of 0.052 MHz. The frequency shift between the  $N = 1$  peak and the Rb line can be measured in the same way, and the free spectral range (FSR) of the ULE-FPI was determined from the frequency difference between these two locking positions. From the statistical distribution of over 7000 measurements (Fig. 2), a most probable value of 1497.028 63(39) MHz was obtained for the FSR near 795 nm. The differences of the FSR values measured at some other wavelengths between 772 and 795 nm have been determined to be less than 0.7 kHz. Combined with the available atomic line references, a sub-megahertz absolute frequency accuracy has been achieved over this spectral range.

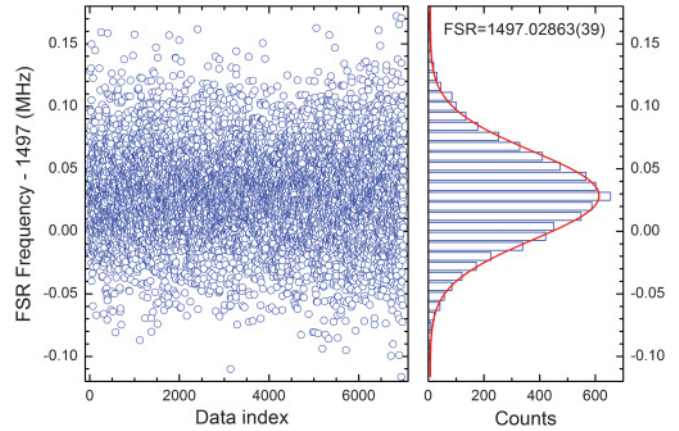


FIG. 2. (Color online) Determination of the free spectral range of the ULE-FPI near 795 nm. Values from over 7000 measurements are shown in the left panel, and the Gaussian profile fitting of the histogram together with the resulted FSR value are given in the right.

The hydrogen rovibrational transitions show significant Dicke narrowing of the line profile with increasing pressure [13–15,19]. As a result of the collision effects, the profile cannot be reproduced by the conventional Voigt line shape. In this work, we adopt the “soft” collisional Galatry model [20] to take into account the effects of Doppler broadening, Dicke narrowing, and collision broadening. The Galatry model was also applied in the study of the first overtone band of  $H_2$  [13,19]. The Gaussian width was fixed at the calculated Doppler width value in the fitting procedure. As illustrated in Fig. 3, the  $S(3)$  line profile recorded at 755 Torr is reproduced within the experimental accuracy, the residuals of the fit being at the experimental noise level. From the fitting of the spectra recorded at different  $H_2$  sample pressures, we obtained the line positions. The pressure-shifted  $S_3(3)$  line positions displayed in Fig. 3(c) show a clear linear dependence with the pressure. A

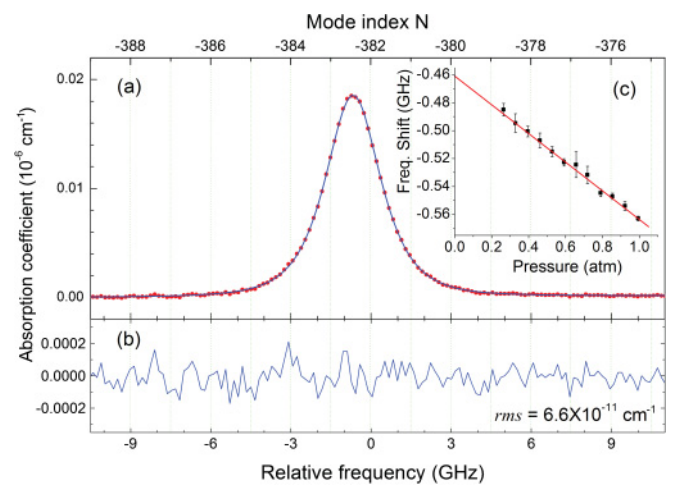


FIG. 3. (Color online) (a) The  $S(3)$  line of  $H_2$  near 796 nm recorded at 755 Torr. Scattered circles: observed spectrum; continuous line: simulated spectrum using a Galatry profile. (b) Residuals between the observed and simulated spectra ( $rms = 6.6 \times 10^{-11} \text{ cm}^{-1}$ ). (c) Center positions (relative to the  $N = -382$  longitudinal modes of the ULE-FPI) at different  $H_2$  sample pressures.

TABLE I. Absolute frequency of the  $S(3)$  line at 796.2 nm and the uncertainty budget (in MHz).

	Value	Uncertainty
Rb line frequency <sup>a</sup> , $\nu_{\text{Rb}}$	377 104 389.803	0.079
$\nu_0 - \nu_{\text{Rb}}$	-247.438	0.052
FSR of ULE-FPI, $f_{\text{FSR}}$	1497.028 63	0.000 39
$\nu_N - \nu_0 = N f_{\text{FSR}}$ , <sup>b</sup>	-571 864.94	0.15
$\nu_{S(3)} - \nu_N$	-459.3	1.6
$\nu_{S(3)}$	376 531 818.1	1.6

<sup>a</sup>Frequency of the  $|5\ ^2S_{1/2}, F=2\rangle \rightarrow |5\ ^2P_{1/2}, F'=1\rangle$  line of  $^{87}\text{Rb}$ , from Ref. [21].

<sup>b</sup> $\nu_0$  and  $\nu_N$  ( $N = -382$ ) are the frequencies of the ULE-FPI transmission modes close to the Rb line and the  $S(3)$  line, respectively.

linear fit yields the line position at zero pressure limit together with the pressure shift coefficient.

The line position of the  $S_3(3)$  line at zero pressure limit is determined to be  $-459.3 \pm 1.6$  MHz relative to the  $N = -382$  mode frequency  $\nu_N$  of the ULE-FPI. The pressure shift coefficient is determined to be  $-104(2)$  MHz/atm (296 K). As shown in Table I, the absolute frequency of the  $^{87}\text{Rb}$   $|5\ ^2S_{1/2}, F=2\rangle \rightarrow |5\ ^2P_{1/2}, F'=1\rangle$  line at 377 104 389.803(79) MHz [21] was first transferred to the  $N = 0$  transmittance mode position of the ULE-FPI, and then to other modes using the accurately determined FSR value. In this way, the absolute frequency of the  $S(3)$  line is determined to be 376 531 818.1  $\pm$  1.6 MHz. The uncertainty budget is included in Table I. The obtained  $S(3)$  line frequency agrees perfectly with the theoretically calculated value where QED corrections are included [9]. The  $(\nu_{\text{obs}} - \nu_{\text{calc}})$  difference is only  $3.2 \times 10^{-4}$   $\text{cm}^{-1}$  (9.6 MHz), which is considerably smaller than the claimed theoretical accuracy (75 MHz in this region) [13]. As a comparison, the overall relativistic and QED contributions calculated for the ( $V = 3, J = 5$ ) upper energy level is 0.7365  $\text{cm}^{-1}$  [9]. After correction of the  $S(3)$  position given by Bragg *et al.* [14] using the pressure shift coefficient obtained above, the resulted line center agrees with our value within the claimed uncertainty of the FTS measurements ( $5.9 \times 10^{-3}$   $\text{cm}^{-1}$ ). Figure 4 illustrates the gain achieved on the precision on the  $S(3)$  position, compared to the calculations [9] and to the FTS measurement by Bragg *et al.* [14].

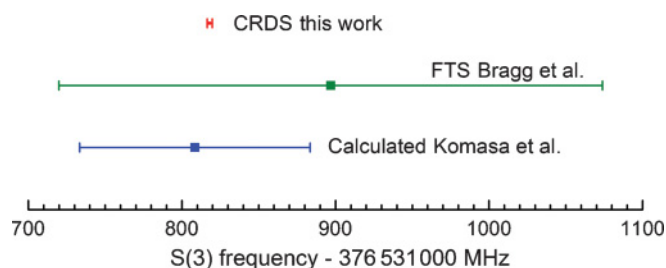


FIG. 4. (Color online) Comparison of the calculated and observed positions of the  $S(3)$  line. The position from Bragg *et al.* [14] is shown after correction of pressure shift. Calculated value is from Ref. [9,13].

The high sensitivity of the CRDS technique has allowed us to determine accurate values of the line parameters of the very weak electric-quadrupole transitions of the second overtone band of  $\text{H}_2$ . The absolute frequency of the  $S_3(3)$  transition was determined to be 12 559.749 52(5)  $\text{cm}^{-1}$  (relative accuracy  $4 \times 10^{-9}$ ), which is the most precisely determined position for a  $\text{H}_2$  transition from the ground electronic state. The difference between this value and the theoretical calculation including QED corrections [9] is one order of magnitude smaller than the claimed uncertainty of the calculations. This agreement indicates that the  $\alpha^4$  and higher-order QED corrections have been well estimated in the calculations ( $\alpha$  is the fine structure constant). The accuracy on the experimental frequency can be further improved to the kilohertz level by locking a cavity ring-down spectrometer to a set of frequency combs [18]. Such high-precision studies of the rovibrational transitions of the hydrogen molecule will provide an ideal test for high-level quantum chemistry calculations. Further studies in such a simple molecular system may shed new light on the test of the QED theory and the determination of physical constants such as the proton-to-electron relative mass.

The authors thank Z.-T. Lu for carefully reading the manuscript and for helpful suggestions. This work is jointly supported by NSFC (90921006, 20903085, and 20873132), NKBRSF (2007CB815203 and 2010CB923300), and FRFCU. The support of the Groupement de Recherche International SAMIA between CNRS (France) and CAS (China) is also acknowledged.

- [1] K. Piszczatowski, G. Lach, M. Przybytek, J. Komasa, K. Pachucki, and B. Jezierski, *J. Chem. Theory Comput.* **5**, 3039 (2009).
- [2] Y. P. Zhang, C. H. Cheng, J. T. Kim, J. Stanojevic, and E. E. Eyler, *Phys. Rev. Lett.* **92**, 203003 (2004).
- [3] J. Liu, E. J. Salumbides, U. Hollenstein, J. C. J. Koelemeij, K. S. E. Eikema, W. Ubachs, and F. Merkt, *J. Chem. Phys.* **130**, 174306 (2009).
- [4] D. Sprecher, J. Liu, C. Jungen, W. Ubachs, and F. Merkt, *J. Chem. Phys.* **133**, 111102 (2010).
- [5] J. Liu, D. Sprecher, C. Jungen, W. Ubachs, and F. Merkt, *J. Chem. Phys.* **132**, 154301 (2010).
- [6] D. Sprecher, C. Jungen, W. Ubachs, and F. Merkt, *Faraday Disc.* **150**, 51 (2011).
- [7] K. Pachucki and J. Komasa, *J. Chem. Phys.* **130**, 164113 (2009).
- [8] K. Pachucki and J. Komasa, *Phys. Chem. Chem. Phys.* **12**, 9188 (2010).
- [9] J. Komasa, K. Piszczatowski, G. Yach, M. Przybytek, B. Jezierski, and K. Pachucki, *J. Chem. Theory Comput.* **7**, 3105 (2011).
- [10] E. J. Salumbides, G. D. Dickenson, T. I. Ivanov, and W. Ubachs, *Phys. Rev. Lett.* **107**, 043005 (2011).
- [11] E. Reinhold, R. Buning, U. Hollenstein, A. Ivanchik, P. Petitjean, and W. Ubachs, *Phys. Rev. Lett.* **96**, 151101 (2006).

- [12] G. Herzberg, *Nature* **163**, 170 (1949).
- [13] A. Campargue, S. Kassi, K. Pachucki, and J. Komasa, *Phys. Chem. Chem. Phys.* **14**, 802 (2012).
- [14] S. L. Bragg, J. W. Brault, and W. H. Smith, *Astrophys. J.* **263**, 999 (1982).
- [15] D. Robie and J. Hodges, *J. Chem. Phys.* **124**, 024307 (2006).
- [16] L. Frommhold, *Collision-Induced Absorption in Gases* (Cambridge University Press, Cambridge, 1993).
- [17] B. Gao, W. Jiang, A.-W. Liu, Y. Lu, C.-F. Cheng, G.-S. Cheng, and S.-M. Hu, *Rev. Sci. Instrum.* **81**, 043105 (2010).
- [18] H. Pan, C.-F. Cheng, Y. R. Sun, B. Gao, A.-W. Liu, and S.-M. Hu, *Rev. Sci. Instrum.* **82**, 103110 (2011).
- [19] M. Gupta, T. Owano, D. S. Baer, and A. O'Keefe, *Chem. Phys. Lett.* **418**, 11 (2006).
- [20] L. Galatry, *Phys. Rev.* **122**, 1218 (1961).
- [21] M. Maric, J. J. McFerran, and A. N. Luiten, *Phys. Rev. A* **77**, 032502 (2008).